THE PENNSYLVANIA STATE UNIVERSITY
SCHREYER HONORS COLLEGE

DEPARTMENT OF METEOROLOGY AND ATMOSPHERIC SCIENCE

Analysis of Environmental Factors Contributing to the Eyewall Replacement Cycle of
Hurricanes

MARTHA CHRISTINO
SPRING 2023

A thesis
submitted in partial fulfillment
of the requirements
for baccalaureate degrees
in Meteorology and Atmospheric Science and Civil Engineering with honors in Meteorology and
Atmospheric Science

Reviewed and approved* by the following:

George Young
Professor Emeritus of Meteorology
Thesis Supervisor

Paul Markowski
Distinguished Professor of Meteorology
Honors Adviser

Anthony Didlake
Associate Professor of Meteorology
Faculty Reader

* Electronic approvals are on file.

ABSTRACT

Even the most advanced hurricane forecast models have difficulty predicting eyewall replacement cycles (ERCs) in tropical cyclones. Most research has attempted to solve this problem by working to understand the dynamic and kinematic drivers of an ERC. This project proposes an alternative approach focused on analyzing the changes in measurable environmental factors and utilizing a machine learning algorithm to predict the ERC. The aim of the first phase of this project is to establish which environmental factors are linked to the initial development of a secondary eyewall. Thirty-seven occurrences of secondary eyewall formation (SEF) in hurricanes between 1984 and 2018 were selected based on the criteria used in Sitkowski, et al. (2011). Each SEF event was matched with a similarly intensifying hurricane that did not experience a subsequent SEF event based on the year and storm intensity. Using environmental data from the Statistical Hurricane Intensity Prediction Scheme (SHIPS) predictor files, the change in each environmental variable at six-hour intervals for twenty-four hours before the start of SEF was analyzed. The environmental variables that experience the most significant change prior to SEF will determine which variables should be used as predictors in a machine learning program designed to predict SEF onset. The goal of this research is to create an algorithm capable of predicting a SEF event twenty-four hours in advance. This algorithm will be compared to existing statistical SEF prediction schemes. Predicting ERC events will allow hurricane track and intensity models to produce more accurate forecasts and emergency response centers to accordingly alter evacuation zones, resulting in decreased economic loss and fatalities.

TABLE OF CONTENTS

LIST OF FIGURES

LIST OF TABLES

ACKNOWLEDGEMENTS

I would first like to thank the Penn State faculty and staff that supported me in writing this thesis and throughout my undergraduate career. Dr. Young's guidance in research, academics, and graduate school planning has been invaluable. I would not have completed this thesis or the meteorology and engineering programs without his support. Dr. Markowski has also been pivotal in the completion of this thesis and my graduation as my honors advisor this last year. I am grateful to Dr. Didlake, Alvin Cheung, and Bruno Rojas for making tropical storm dynamics interesting, imparting their knowledge, and answering millions of questions. I also owe a debt of gratitude to Dr. Nese, Amber DeCosmo, Dr. Guler, and Brain Naberezny for keeping my graduation schedule on track. This research would not be possible without the continued support of the staff in the Metrology and Atmospheric Sciences Department, the College of Earth and Mineral Sciences, and the Department of Civil and Environmental Engineering.

I would also like to thank my friends and family for supporting me throughout my college experience. Keely, Lauren, and Hannah for keeping me grounded. My father for setting the example as one of the original University Scholars, and my mother and sister for their undying support.

Chapter 1

Introduction

Accurate forecasting of hurricane intensity changes is essential to protect lives and property in the path of a major storm. Hurricane intensity can change by category on the Saffir-Simpson scale during the Eyewall Replacement Cycle (ERC). Yet, there is no agreed upon reliable method of predicting the ERC. This results in inaccurate intensity forecasts and unpredicted changes in the damage potential of major hurricanes prior to landfall. Therefore, it is imperative that an ERC prediction method be established within the forecasting community.

Research has shown a predictable intensity fluctuation during the ERC in which the inner wind maximum weakens while a secondary wind maximum develops at greater radius and strengthens to overcome the original inner wind maximum and form a new eyewall. During this time there is a documented intensification, weakening, and reintensification pattern (Sitkowski 2011). The image below from Zhou and Wang shows the development of two concentric eyewalls as the outer wind maximum constricts inward to replace the original wind maximum. The moment at which two eyewalls become visible is known as Secondary Eyewall Formation (SEF). The ERC is defined as the entire process of SEF, inward constriction, eyewall replacement, and reintensification that occurs on average over 36 hours.
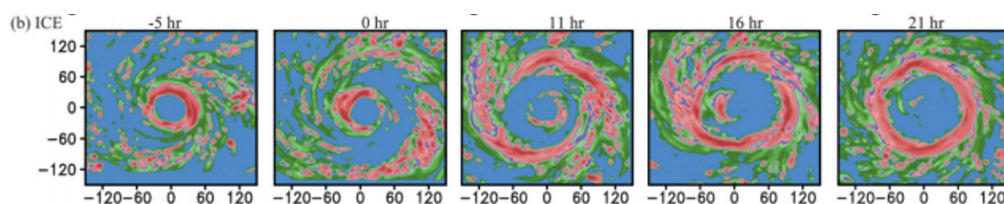
Figure 1. Zhou and Wang (2009) Eyewall Replacement Cycle in Timesteps

There is no denying the significance of this ERC process. It occurs in 72% of major Atlantic hurricanes. Hurricane Andrew 1992 strengthened immediately prior to landfall as a result of the ERC and the large storm surge brought onshore by Hurricane Katrina 2005 can be attributed to a broadening of the wind field during the ERC.

The largest barrier to forecasting the ERC is a lack of understanding of the dynamic, kinematic, and thermodynamic drivers of the ERC. Even with this understanding three major questions remain: why does this process occur, can we predict this process, and how strong will reintensification be?

The majority of published research has worked to address the first of these major questions. Sitkowski (2011) established the identification phases of the ERC linked the onset of the cycle to an increase in integrated kinetic energy. Research has also shown the development of a critical moat region between the original and secondary wind maximums (Sitkowski 2011). Additionally, the internal dynamical processes within the moat region have been shown to dictate the duration of the concentric eyewall formation (Yang 2021). The symmetry of the storm has also been linked to ERC development. Kepert (2013) showed the boundary layer dynamics can be responsible for the enhancement of the radial vorticity gradient. The debate over external versus internal dynamic drivers also includes disagreement on the role of ice particles in secondary eyewall formation (Zhou and Wang 2011).

While disagreement on driving factors of the ERC continues, impacts from the ERC on major hurricanes before making landfall continue to cause destruction. In 2017, destructive Hurricane Irma completed a rapid intensification period consisting of two ERCs prior to landfall (Fisher et al. 2020). As a result, research must address the second major question of prediction even though there is still no consensus on causation.

Kossin (2009) attempted to identify the onset of the ERC using a Bayes probabilistic model and classification scheme. This research showed the importance of several environmental factors including climatological depth of the 26°C ocean isotherm, 200-hPa zonal wind (200-800 km from center), 0-600kn average symmetric tangential wind at 850hPa, azimuthally average surface pressure at outer edge of vortex, and 850-200hPa shear magnitude in ERC identification and prediction.

This paper attempts to build on published research to address the critical question of prediction of the ERC. The presented research aims to determine which environmental factors exhibit statistically significant changes prior in six-hour increments for 24 hours prior to the ERC start time. This work then attempts to utilize the identified factors in a machine learning logistic regression model to predict the ERC. Full results of statistical analysis for variable significance to the ERC will be presented as well as preliminary model results, which show some success at ERC prediction.

Chapter 2

Methods

Data

The start and end time of the ERC case used in this research were defined by flight level aircraft data form the NOAA WP-3D and U.S. Air Force WC-130 aircraft in Sitkowski (2011). Sitkowski (2011) analyzed a dataset of 79 hurricanes from 1977 to 2008, identifying 24 ERC events. Research by Wunsch (2018) following the same determination method as Sitkowski added the remaining thirteen ERC events analyzed in this research to create the 37 ERC cases from 1984 to 2018 considered in this research.

Each of the 37 ERC cases was matched with a point in an intensifying hurricane that did not produce an eyewall replacement cycle. It is important to note that, while the methodology of defining ERC start and end times is consistent across the analyzed data, there is implicit uncertainty in these times which may introduce error. For this paper, an ERC/non-ERC (or positive/negative) point will be considered the full length of the ERC case or the selected non-ERC case.

Only storms that reached hurricane level intensity are analyzed in Sitkowski (2011), Wunsch (2018), and this research. This is due to data availability and the need to keep consistency within the created data set for machine learning training. Additionally, all the ERC points considered occurred with the storm was over water. This ensures land atmosphere interactions will not skew data or otherwise render it unfit for statistical analysis.

The environmental data used in this research is from the Statistical Hurricane Intensity Prediction Scheme (SHIPS) dataset. The SHIPS model provides intensity forecasts based on

linear regression techniques. There are 89 environmental predictors available. 75 of these factors were analyzed across all 74 ERC positive/negative cases.

Point Matching

To create the list of 74 positive and negative ERC points, each identified positive ERC point from previous research was matched with a negative ERC point. This matching is essential to creating a data framework that can evaluate significant differences between positive and negative ERC occurrences.

Negative storm points were selected exclusively from intensifying storms – storms in which the maximum surface winds were increasing by at least 10 knots in the 12 hours prior to the storm point. Additionally, negative storm points were selected to have the same Saffir-Simpson category as and have occurred in the same year as the corresponding positive point. If a storm of the same category in the same year without an ERC did not exist, a storm within two years and one category of the positive point storm was chosen.

The table below shows all positive and negative ERC points in their matched order.

Table 1. Matched Positive and Negative ERC Points

Positive and Negative ERC points matched based on storm intensification of at least 10kt/12hr, Saffir-Simpson storm category, and year.

Positive ERC Occurrence Start Times	Negative ERC Occurrence Start Times
DIAN 840911 12	GLOR 850921 12
LUIS 950905 00	FELI 950812 06
LUIS 950906 12	OPAL 951002 06
ERIK 970908 18	BONN 980823 12
GEOR 980919 18	BRET 990821 06
FLOY 990911 06	BRET 990820 00

FLOY 990912 18	LENN 991117 06
GERT 990917 06	LENN 991115 06
ERIN 010910 12	FELI 010913 18
MICH 011103 12	IRIS 011007 00
ISID 020919 18	KATE 031003 06
FABI 030903 18	KARL 040917 00
ISAB 030915 18	LILI 021001 18
FRAN 040830 06	KARL 040918 18
FRAN 040830 18	KARL 040919 18
FRAN 040901 06	KATE 030928 06
FRAN 040903 18	KATE 031001 18
IVAN 040908 18	CHAR 040810 18
IVAN 040909 18	KARL 040923 06
IVAN 040910 18	CHAR 040811 18
IVAN 040912 12	CHAR 040812 18
KATR 050826 18	EMIL 050713 18
KATR 050828 12	EMIL 050716 12
RITA 050921 18	EMIL 050714 18
WILM 051018 18	EMIL 050719 00
HELE 060919 00	GORD 060914 00
DEAN 070818 06	GUST 080826 06
DEAN 070819 00	GUST 080828 18
FELI 070903 12	IKE 080907 00
BERT 080710 06	FRED 090909 06
MATT 161001 06	NICO 161006 12
MATT 161006 12	NICO 161012 06
HARV 170824 12	JOAQ 150930 18
IRMA 170904 00	JOSE 170907 00
IRMA 170907 12	JOSE 170908 18
MARI 170923 12	MICH 181009 06
FLOR 180910 12	OPHE 171013 00

Average Change

The change in each environmental variable over six-hour periods of the day leading to the

ERC start time provided the factor data analyzed for this research. For example, the change in

surface wind velocity between 12-18 hours prior to an ERC start time was compared between the

positive and negative ERC points to determine significance in relation to the ERC. Since the data

is only reported every six hours, this paper refers to the six-hour change value as the "average change."

Average change values were calculated for the 0-6hr, 6-12hr, 12-18hr, and 18-24hr time periods prior to each ERC start time for each environmental predictor. These values were then used in statistical significance testing and for machine learning model training.

Variable Eliminations

Several of the environmental factors available in the SHIPS data were not considered in this analysis because of incomplete data or formatting differences in the data. Ocean depths of the 30 through 16-degree Celsius isotherms, ocean heat content from satellite date and at the 20-degree isotherm, depth of the maximum ocean temperature, climatological values of the NCODA variables, max ocean temperature in the NCODA variable profile, depth of the mixed layer, and depth and temperature of the lowest model levels in the NCODS analysis were not included in this analysis. Moreover, ocean heat content and sea surface temperature from the NCODA analysis and principle components from IR imagery 1.5hours before initial time were analyzed for fewer than the nominal 37 cases due to outliers in the data.

Analysis Procedure

A standard independent two sample T-test that assumed equal population variances was used in comparing positive and negative ERC point data. After the average change for each environmental variable and time period was calculated the positive and negative ERC points were compared. For each environmental variable and time-period combination, the average

change of the 37 positive cases was tested against the average change of the 37 negative cases to

determine the statistical significance of each variable in each timer-period to ERC occurrence.

The null hypothesis for each T test was that the arithmetic means of average

change in the environmental variable during the assigned time-period in the positive and

negative ERC cases were identical. Therefore, accepting the null hypothesis would be

acknowledging that the environmental variable being tested has no impact on the occurrence of

the ERC in the timer period under evaluation. Rejecting the null hypothesis would indicate that

the environmental variable in question may be helpful in predicting the ERC during the tested

time-period.

The P statistics of the T tests were compared between factors. The p-value is

determined by comparing the t-statistic against a theoretical t distribution assuming a normal

distribution of the data. In this analysis, the p-value is used as an indicator of the reliability of the

t-statistic to determine the likelihood of chance in the calculated T value. The p-value threshold

accepted as reasonable will be discussed further in results, but it is important to note that the

relatively small sample size of ERC data will impact the average value of the p-value across all

completed T tests.

Machine Learning

The SciKit-Learn implementation of the logistic regression machine learning model was

used to create an ERC prediction model based on the identified environmental factors. In all runs

of the model predictor data was fed into the model and a true/false binary ERC predictand was

the model output. Prior to identification of the significant environmental factors, the logistic

regression model was tested with random data to determine the number of predictors that could be used before the model developed false skill.

Randomly generated data was created for 54 environmental predictors. The model was then trained with this random data as predictors and a combination of 37 negative/positive randomly assigned ERC binary cases as the predictand. 37 additional negative/positive randomly assigned binary ERC cases were then used and predictands to test the model with secondary randomly generated data as predictors. The number of predictors used in the model training and testing was increased until the model developed entirely false skill. The limited number of ERC cases available for training/testing data is the limiting factor in the number of predictors that can be used for model development without attaining false model skill.

After analysis of the critical number of predictors to preclude false skill development and identification of the significant environmental factors, the logistic regression model was trained and tested with the SHIPS environmental data. The ERC cases were split into a training group and a testing group. The data used to train the model includes 19 positive ERC predictand cases and 18 negative ERC predictand cases. The data used to test the model skill for each model run utilizes the remaining 18 positive ERC predictand and 19 negative ERC predictand cases.

The model used for the results in this report works with four predictors selected by the user in a single time frame (time frames being 6-0hr, 12-6hr, 18-12hr, and 24-18hrs in advance of the ERC start time). The program calculates the average change in each predictor for the assigned time frame. Consequently, the program creates a training matrix of the average change in each predictor variable across the 37 training ERC cases to feed into the logistic regression model.

The testing data is created in an identical manner; a combined matrix of the average change for each predictor variable is generated across the 37 ERC test cases. Model results from this testing data are then compared with the assigned binary predictand values. The number of current ERC predictions to total predictions made is then calculated and output in the skill score.

The model parameters used on the logistic regression model are as follows. The L2 penalty term was used with liblinear as the solver due to the size of the dataset. Dual formulation was not used in the model because the number of samples greatly exceeded the number of features. All other default model parameters were used.

Chapter 3

Results

Environmental Factor Analysis

Each time frame revealed a different set of environmental factors significant to the ERC when tested via the two sample t-test approach. While some environmental factors did appear as significant across multiple time frames, the most correlated variable in both the positive and negative directions were unique to each time frame. All environmental variable names are given in the appendix. This is shown in Table 2, where the individual largest positive and negative T statistics are reported for each time frame. Noticeably, there is no consistent pattern on where the largest positive or negative statistic is more significant.

Table 2. Summary Results for Significant Environmental Factors Across All Time Frames

No repeated factors for largest positive or negative statistic across time frames. All time frames given are in hours prior to ERC/non-ERC start time. VMAX and DELV share the same negative statistic magnitude in the 18-12hr time frame.

Time Period	Largest Positive T Statistic Factor	Positive T Statistics Magnitude	Largest Negative T Statistic Factor	Negative T Statistic Magnitude
6-0hr	TGRD	2.03	U200	2.13
12-6hr	V850	3.75	SHRG	2.07
18-12hr	T000	1.88	VMAX/DELV	2.26
24-18hr	PEFC	2.70	REFC	2.10

The results from each time frame further reveals a lack of similarity in significant factors across time frames. While the 0-6hr time frame can only be used for ERC diagnosis, not

prediction, it is still relevant for analysis of significant environmental factors when compared to data from the adjacent 6-12hr time frame. Notably, the only one environmental variable is repeated between the top five highest positive/negative statistics in the 6-0hr and 12-6hr time frames. This variable is the 200hPa zonal wind vs. time for a radius of 0-500km, as seen in Table 3 and Table 4.

Table 3. Significant Environmental Factors Based on 6-0hr Average Change

The average change in environmental factors from 6 hours prior to the start of the ERC. The top two positive and negative statistics show strong trends with small chance of randomness. This data would be used for diagnosis of an occuring ERC, not prediction of future ERC events.

Largest Positively Correlated Factors	Largest Positive T Statistic	Positive T Statistics Magnitude	Largest Negative T Statistic	Negative T Statistic Magnitude	P Value
TGRD	2.03	0.05	U200	2.13	0.04
TADV	1.92	0.06	PC00	1.91	0.06
VMFX	1.86	0.07	U20C	1.56	0.12
VVAV	1.78	0.08	PCM1	1.52	0.13
RHLO	1.67	0.10	SHRD	1.45	0.15

As the p value column in tables 3 – 6 verify, despite the small data set all reported significance values have a relatively low chance of randomness. In most cases the p value is less than 10%. Only 13 of the 40 significant variable results presented show a p value at or above 10%, the highest p value represented in the top five T statistics is 21%. These values must be contextualized given the sample size of the data.

Table 4. Significant Environmental Factors Based on 12-6hr Average Change

12-6hr data based on the average change t-test. This time frame displays the least uncertainty in positively correlated factors.

Largest Positively Correlated Factors	Largest Positive T Statistic	Positive T Statistics Magnitude	Largest Negative T Statistic	Negative T Statistic Magnitude	P Value

V850	3.75	0.0004	SHRG	2.07	0.04
T150	2.5	0.01	CFLX	1.73	0.09
RHMD	2.45	0.02	SHRD	1.69	0.09
PC00	2.35	0.02	G200	1.56	0.12
TWAC	2.2	0.03	U20C	1.55	0.13

The 6-12hr significance data displays the most certainty in positively correlated factors across all tested time frames. None of the 12-6hr top five positive T statistics align with the top five positive statistics established for the 0-6hr time frame, the 18-12hr time frame, or the 24-18hr time frame. As mentioned previously the U20C variable does appear as a negative statistic in both the 12-6hr and 6-0hr time frames. CFLX – the dry air predictor, appears with a strong negative statistic in the 12-6hr time frame and the 18-12hr time frame.

Table 5. Significant Environmental Factors Based on 18-12hr Average Change

Five new significant positive statistic factors and four new significant negative statistic factors are introduced in the 18-12hr time frame.

Largest Positively Correlated Factors	Largest Positive T Statistic	Positive T Statistics Magnitude	Largest Negative T Statistic	Negative T Statistic Magnitude	P Value
T000	1.88	0.06	VMAX	2.26	0.03
G250	1.88	0.07	DELV	2.26	0.03
Z850	1.81	0.07	V20C	2.07	0.04
G150	1.61	0.11	CFLX	1.63	0.11
E000	1.51	0.15	R000	1.61	0.11

Besides the CFLX similarity with the 12-6hr data, the 18-12hr significance data introduced new factors for consideration in relation to ERC development. The highest average

uncertainty in positively correlated factors occurs in this time frame, as made clear in the listed p

values. In the negative statistics, the maximum surface wind speed and the intensity scale factor

show identical strength statistics and chance of uncertainty.

Table 6. Significant Environmental Factors Based on 24-18hr Average Change

The furthest time frame from the ERC point displays strong positive statistics with little uncertainty. Yet, this time frame displays the most uncertain negative statistics across the presented data.

Largest Positively Correlated Factors	Largest Positive T Statistic	Positive T Statistics Magnitude	Largest Negative T Statistic	Negative T Statistic Magnitude	P Value
PEFC	2.70	0.009	REFC	2.10	0.04
V500	2.27	0.03	D200	1.80	0.08
O500	2.04	0.05	U200	1.35	0.18
V300	2.02	0.05	OAGE	1.35	0.18
DSTA	1.73	0.09	EPOS	1.26	0.21

In the time frame furthest from the ERC start point, ten new factors significant to ERC

occurrence are identified. There is low uncertainty in the presented positive T statistics and high

uncertainty in the presented negative statistics. The p values in the negative case are of the

largest in magnitude found in the data set, indicating uncertainty. The contribution of eddy fluxes

both positively and negatively is worthy of note. Planetary eddy momentum flux convergence

gives the strongest and most certain positive statistic, while relative eddy momentum flux

convergence is a strongly negative difference between the ERC and non-ERC mean.

A summary of all the environmental factors tested and the T statistic values

established for each across all time frames can be seen in Figure 1. Environmental factors which

showed consistently strong differences across time frames, even if not in the top five, include

longitude (LON), 850hPa vorticity (Z850), heading above shear vector (SDDC), longitude of

850hPa vortex center (TLON), and tangential winds at 300hPa (V300).

Figure 2. Graph of T Statistics Across All Environmental Factors and Time Frames

Figure showing all tested T statistic values. Note the agreement across all time frames of the significance of the average change in longitude, 850hPa vorticity, and longitude of the 850hPa cortex center.

Machine Learning Prediction

The SHIPS data set used provides more predictors than there are ERC cases to train and test a machine learning model against. Therefore, the number of predictors needed to generate false skill in a logistic regression model was tested and can be seen in Figure 3. Based on the results of this testing, only four predictors were used in the initial training and testing of the regression model presented in this paper.

Figure 3. Results of Random Data Skill Testing

The results presented in this figure show that false model skill is quickly developed after more than 8 predictors are utilized. Using two to four predictors greatly reduces the chance of false skill development but does not eliminate it.

For the preliminary run of the model, the four environmental factors with the highest differences in ERC and non-ERC means were selected and tested. The results of this model run can be seen in Table 7. Based on the results displayed in Figure 3, the machine learning model develops false skill quickly as the number of predictors increases. For this study the number of predictors was limited to four because the average false skill developed remains under 0.60 while still allowing multiple environmental factors to be considered by the algorithm.

Table 7. Preliminary Model Run Results

Early model results based on the four highest T statistic factors show increasing skill the closer to ERC event.

Predictors	Time Period	Mean Model Accuracy
PEFC, V500, REFC, O500	24-18hr	0.62
VMAX, DELV, V20C, T000	18-12hr	0.68
V850, T150, RHMD, PC00	12-6hr	0.78

Chapter 4

Discussion

These preliminary model results do show some skill at predicting the ERC using machine learning methods. However, the success of the machine learning model is entirely dependent on the effectiveness of the identified predictors at creating a clear delineation between ERC negative and positive events. Fischer (2019) clearly establishes the link between ERC and environmental factors and the need for further investigation. The lack of repeated factors identified as significant across the time frames presents the need for unique prediction

considerations for each six-hour time frame before an ERC event. The certainty of each statistic

most also be accounted for in relation to the overall small sample size of the data considered.

The significant differences in variable relevance between periods displays that

there are multiple distinct phases leading up to an ERC occurrence. This supports research by

Sitkowski (2011), which argued distinct intensification, weakening, and re-intensification phases

in the ERC process. The weakening phase can be clearly seen in the data from this experiment

during the 18-12hr time frame. The negative difference to ERC occurrence with both max

surface wind speed and the intensity factor displayed during this time frame show agreement

with Sitkowski's analysis of Hurricane Dorian's weakening period prior to ERC occurrence.

Willoughby (1981) also showed a weakening period, which would agree with the negative T

statistics presented here.

Overall, the negative T statistics dominate over the positive statistics in this 18-

12hr time frame. This does not hold as the ERC start time approaches. In the 12-6hr time frame

the positive difference in means far outweighs the negative difference in significance. The

impact of thermodynamic factors seem to become important during this time frame as factors

related to temperature and humidity begin to rival the importance of dynamic tangential wind

and vorticity factors. The importance of these dynamic factors at the beginning of the ERC

process are well documented by Abarca (2013). Putting these two time periods together, we can

begin to construct a picture of the ERC where a weakening event in the 18-12hr time frame

leaves the storm susceptible to more thermodynamic factors in the 12-6hr period before an ERC

event.

The significance of eddy momentum flux convergence displayed in the 24-18hr

time frame does not contradict published research, yet it is not in strong agreement either. This

early ERC thermodynamic driver could connect to deeper storm dynamics related to global heat transport and locations of convective heat sources. The certainty of the planetary eddy momentum flux convergence statistic demands attention and the dichotomy of the positive planetary convergence with a negative relative convergence presents an interesting case. More research on this component will need to be done before conclusive statements can be made on the subject.

Besides the factors selected because of high positive/negative statistics in each time frame, it is also important to analyze the factors that appeared consistently across time frames even with smaller magnitude differences in the means. One of these interesting statistics is the average change in longitude. The average change in longitude appears to be most significant in the 24-18hr time frame but holds a positive difference in means across all time frames. Figure 4 contains the tracks of several major hurricanes, some with and some without ERC events. This figure demonstrates that hurricanes with multiple ERC events have tracks which parallel latitudinal lines.
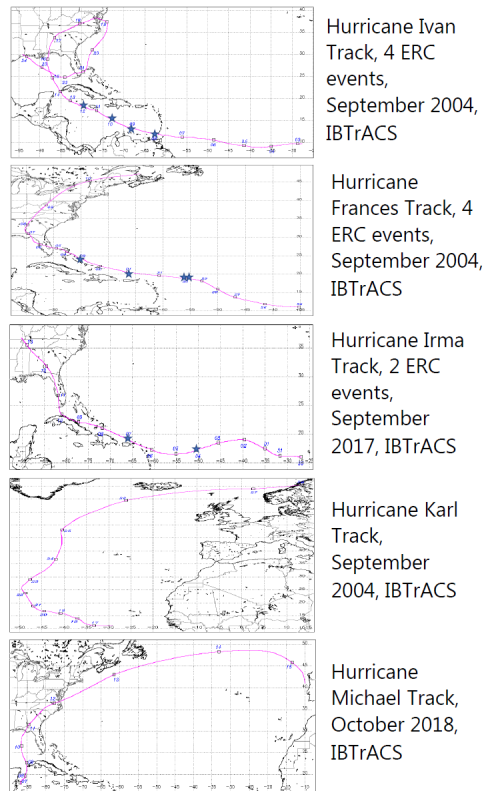
Figure 4. Hurricane Track Comparison for ERC and non-ERC Major Hurricanes

Analysis of tracks from major hurricanes with and without ERC events, shows correlation between a lack of longitudinal movement and ERC occurrence. All tracks from IBTrACS.

The impact of northward motion on ERC occurrence was also noted in Yang (2021). Yang (2021) found that long-lived concentric eyewall formations occurred more frequently in tropical cyclones with smaller northward motion components. This could be due to a variety of factors including sea surface temperatures, atmospheric moisture, blocking patterns at time of storm development, and should be further investigated. Kossin (2009) found a link between SEF and latitude, possibly indicating that ERCs are more likely further south.

Kossin (2009) constructed a Bayesian model to identify SEF events and several features found relevant to SEF formation agree with the identified significant factors for ERC development. The 200hPa zonal wind was identified as a possible predictor variable by both

Kossin (2009) and this study. This study specifically showed 200hPa zonal wind as a significant factor in the 6-0hr and 24-18hr time frames. The Bayesian probabilistic model was focused on SEF identification, therefore links between significant environmental factors in the 6-0hr analysis in this study and the features used by Kossin (2009) are expected. 850-200hPa shear magnitude was also used in Kossin (2009) and identified in the 6-0hr time frame of this study.

Other factors found in this study and used in Kossin (2009) were similar, though not identical like zonal winds and shear magnitude. The Bayesian model utilized current intensity as a predictor and this study identified intensity change as a significant indicator of ERC occurrence in the 18-12hr time frame. Additionally, relative humidity (%) vs time (200-88km) for 700-500hPa was identified as a significant variable in the 12-6hr time frame of this study. Kossin (2009) also used relative humidity as a model feature but considered the 500-300hPa level. Tangential wind factors were also used in this study and Kossin (2009). This study identified the tangential wind azimuthally averaged at r=500km as significant at the 500hPa level for the 24-18hr time frame and at the 850hPa level for the 12-6hr time frame. Similarly, Kossin (2009) used the 0-600om average symmetric tangential wind at 850hPa from NECP analysis. Of note, both Kossin (2009) and Sitkowski (2011) also identified infrared imagery as a method of identifying SEF and an infrared imagery related variable (PC00) was shown as significant in the 12-6hr time frame of this work.

The preliminary machine learning model results do show promise in prediction ability of the ERC given environmental predictors. This is well shown in the 12-6hr time frame, where there is a starting accuracy of 78% with predictors chosen simply based on high T statistics. A jackknife method of testing the machine learning model where all but N cases are used to train, and the model is continuously re-built and tested should be used in the future to further test the

model accuracy. More careful predictor selection coupled with post-processing will likely improve this model's accuracy. Kossin (2009) was able to achieve a ~88% accuracy for SEF identification using a Bayesian probabilistic model. Machine learning preliminary model data which is only 10% less accurate than the Bayesian model in the 6 hours out time frame, dictates further consideration of the machine learning model for ERC prediction.

Chapter 5

Conclusions

The preliminary accuracy of the machine learning model shows promise in comparison to and the identified significant environmental factors agree with published work. Which factors are significant in ERC development were identified within each time frame. Furthermore, the lack of consistency in environmental factors repeated across time frames was contextualized to the understanding of distinct sections in ERC development from published research.

The next major challenge in continuing this research is to further develop the machine learning algorithm to increase the accuracy of ERC prediction across all time periods. Balancing positive and negatively correlated factors as predictors or strategically selecting the number of negatively vs. positively correlated factors instead of selection of the largest magnitude T statistics should be the first step of this effort. Integrating factors with notable statistics across all time frames could also increase model accuracy.

While the preliminary model run was completed with four predictors, decreasing to three or increasing to between five and seven predictors may also be valid and increase model skill. However, when increasing the number of predictors, preventing the development of false model skill will become a serious consideration. The limited number of positive ERC points available puts a serve constraint on the number of predictors used and model complexity. If the ERC proves to be more complex than the number of predictors used in this model can accurately represent, more data will be needed to make progress in ERC prediction via machine learning algorithm.

       The overall goal of this research was to identify the environmental factors significant in ERC formation with the eventual goal of predicting the ERC utilizing machine learning. A comprehensive list of significant environmental factors for the 6-0hr, 12-6hr, 18-12hr, and 24-18hr time frames was created and explained, meeting this initial goal. Moreover, the preliminary success of the machine learning algorithm when using the identified environmental factors as predictors, further proves the success of significant factor identification. This work opens the door for future prediction of the ERC using environmental data and machine learning methods.

Appendix A

SHIPS Predictor Information

Table 8. SHIPS Predictor Full Descriptions

Predictor Abbreviation	Full Predictor Description (Edited from SHIPS Predictor File) _
CD20	Climatological depth (m) of 20 deg C isotherm from 2005-2010 NCODA analyses.
CD26	Same as CD20 for the 26 deg C isotherm.
CFLX	Dry air predictor based on the difference in surface moisture flux between air with the observed (GFS) RH value, and with RH of air mixed from 500hPa to the surface.
COHC	26 deg C ocean heat content (kJ/cm2).
CSST	Climatological Sea Surface Temperature – SST - (deg C * 10) vs time.
D200	850hPa vorticity (sec-1 * 10**7) vs time (r=0-1000 km) for 200hPa divergence.
DELV	Intensity change (kt) -12 to 0, -6 to 0, 0 to 0, 0 to 6, ... 0 to 120 hr.
DIVC	Same as D200 but centered at 850hPa vortex location.
DSST	Daily Reynolds SST (deg C*10) vs time.
DSTA	Same as DSST, but spatially averaged over 5 points (storm center, + 50 km N, E, S and W of center).
DTL	Distance to nearest major land mass (km) vs time.
E000	1000 hPa theta_e (r=200-800 km) vs. time (deg K*10).
ENEG	Same as EPOS, but only negative differences are included. The minus sign is not included.
ENSS	Same as ENEG, but the parcel theta_e is compared with the saturated theta_e of the environment.
EPOS	The average theta e difference between a parcel lifted from the surface and its environment (200-800 km average) versus time (deg C * 10). Only positive differences are included in the average.
EPSS	Same as EPOS, but the parcel theta_e is compared with the saturated theta_e of the environment.
G150	Temperature perturbation at 150hPa due to the symmetric vortex calculated from the gradient

	thermal wind. Averaged from r=200 to 800 km centered on input lat/lon (not always the model/analysis vortex position). (deg C*10)
G200	G150 for 200hPa.
G250	G150 for 250hPa.
HE05	HE07 from P=1000 to 500hPa.
HE07	Storm motion relative helicity (m^2/s^2)*10 for p=1000 to 700hPa, r=200 to 800 km.
INCV	Intensity change (kt) -18 to -12, -12 to -6, ... 114 to 120 hr.
LAT	Latitude
LON	Longitude.
MSLP	Minimum Sea Level Pressure in hPa.
NAGE	Same as OAGE but normalized by the maximum wind/100kt. If the max wind was a constant 100 kt over its past history, NAGE=OAGE.
NOHC	Ocean heat content from the NCODA analysis (J/kg-deg C) relative to the 26 C isotherm.
NSST	SST from the NCODA analysis (deg C*10).
O500	Pressure vertical velocity (hPa/day) at 500hPa, averaged from r=0 to 1000 km.
O700	Same as O500 at 700hPa
OAGE	Ocean Age (hr*10), which is the amount of time the area within 100 km of the storm center has been occupied by the storm along its track up to this point in time.
PC00	Principal components and related variables from IR imagery at t=0.
PCM1	Same as PC00 but for 1.5 hours before initial time.
PCM3	Same as PC00 but for three hours before initial time.
PEFC	Planetary eddy momentum flux convergence (m/sec/day, 100-600 km avg) vs time.
PENC	Azimuthally averaged surface pressure at outer edge of vortex ((hPa-1000)*10).
PENV	200 to 800 km average surface pressure ((hPa-1000) *10).
R000	1000hPa relative humidity (200-800 km average)
REFC	Relative eddy momentum flux convergence (m/sec/day, 100-600 km avg) vs time.
RHHI	Same as RHLO for 500-300hPa.
RHLO	850-700hPa relative humidity (%) vs time (200-800 km).
RHMD	RHLO for 700-500hPa
RSST	Reynolds SST (deg C*10) vs time. Number after SST label is the age in days of the SST analysis used to estimate RSST.

SDDC	Heading (deg) of above shear vector. Westerly shear has a value of 90 deg.
SHDC	Same as SHRD but with vortex removed and averaged from 0-500 km relative to 850hPa vortex center.
SHGC	Same as SHRG but with vortex removed and averaged from 0-500 km relative to 850hPa vortex center.
SHRD	850-200hPa shear magnitude (kt *10) vs time (200-800 km).
SHRG	Generalized 850-200hPa shear magnitude (kt *10) vs time (takes into account all levels from 1000 to 100hPa.
SHRS	850-500hPa shear magnitude (kt *10) vs time.
SHTD	Heading (deg) of above shear vector. Westerly shear has a value of 90 deg.
SHTS	Heading of above shear vector
T000	1000hPa temperature (dec C* 10) (200-800 km average).
T150	200 to 800 km area average 150hPa temperature (deg C *10) versus time.
T200	Same as T150 for 200hPa temperature (deg C *10)
T250	Same as T150 for 250hPa temperature (deg C *10).
TADV	The temperature advection between 850 and 700hPa averaged from 0 to 500 km. From the geostrophic thermal wind (deg per sec*10^6).
TGRD	The magnitude of the temperature gradient between 850 and 700hPa averaged from 0 to 500 km estimated from the geostrophic thermal wind (deg C per m*10^7).
TLAT	Latitude of 850hPa vortex center in NCEP analysis (deg N*10).
TLON	Longitude of 850hPa vortex center in NCEP analysis (deg W*10).
TWAC	0-600 km average symmetric tangential wind at 850hPa from NCEP analysis (m/sec *10).
TWXC	Maximum 850hPa symmetric tangential wind at 850hPa from NCEP analysis (m/sec *10).
U200	200hPa zonal wind (kt *10) vs time (r=200-800 km).
U20C	U200 for r=0-500 km.
V000	The tangential wind (m/sec *10) azimuthally averaged at r=500 km from (TLAT,TLON). If TLAT, TLON are not available, (LAT, LON) are used.
V20C	

V300	V000 at 300hPa
V500	V000 at 500hPa
V850	V850 at 850hPa.
VMAX	Same as U20C, but for the v component of the wind.
VMFX	VVAV, but with a density weighted vertical average.
VMPI	Maximum potential intensity from Kerry Emanuel equation (kt).
VVAC	VVAV but with soundings from 0-500 km with GFS vortex removed.
VVAV	Average (0 to 15 km) vertical velocity (m/s * 100) of a parcel lifted from the surface where entrainment, the ice phase and the condensate weight are accounted for. Note: Moisture and temperature biases between the operational and reanalysis files make this variable inconsistent in the 2001-2007 sample, compared 2000 and before.
XDST	Climatological value of the daily Reynolds SST (deg C*10).
Z000	1000hPa height deviation (m) from the U.S. standard atmosphere.
Z850	850hPa vorticity (sec-1 * 10**7) vs time (r=0-1000 km).

BIBLIOGRAPHY

Abarca, S. F., & Montgomery, M. T. (2013). Essential Dynamics of Secondary Eyewall Formation, *Journal of the Atmospheric Sciences*, *70*(10), 3216-3230. Retrieved Feb 19, 2023, from https://journals.ametsoc.org/view/journals/atsc/70/10/jas-d-12-0318.1.xml

Black, M. L., & Willoughby, H. E. (1992). The Concentric Eyewall Cycle of Hurricane Gilbert, Monthly Weather Review, 120(6), 947-957. Retrieved Feb 2, 2022, from https://journals.ametsoc.org/view/journals/mwre/120/6/1520-0493_1992_120_0947_tcecoh_2_0_co_2.xml

Fischer, M. S., Rogers, R. F., & Reasor, P. D. (2020). The Rapid Intensification and Eyewall Replacement Cycles of Hurricane Irma (2017), *Monthly Weather Review*, *148*(3), 981-1004. Retrieved Feb 19, 2023, from https://journals.ametsoc.org/view/journals/mwre/148/3/mwr-d-19-0185.1.xml

Kepert, J. D. (2013). How Does the Boundary Layer Contribute to Eyewall Replacement Cycles in Axisymmetric Tropical Cyclones?, *Journal of the Atmospheric Sciences*, *70*(9), 2808-2830. Retrieved Feb 19, 2023, from https://journals.ametsoc.org/view/journals/atsc/70/9/jas-d-13-046.1.xml

Kossin, J. P., & Sitkowski, M. (2009). An Objective Model for Identifying Secondary Eyewall Formation in Hurricanes, *Monthly Weather Review*, *137*(3), 876-892. Retrieved Feb 2, 2022, from https://journals.ametsoc.org/view/journals/mwre/137/3/2008mwr2701.1.xml

Maclay, K. S., DeMaria, M., & Vonder Haar, T. H. (2008). Tropical Cyclone Inner-Core Kinetic Energy Evolution, *Monthly Weather Review*, *136*(12), 4882-4898. Retrieved Feb 2, 2022, from https://journals.ametsoc.org/view/journals/mwre/136/12/2008mwr2268.1.xml

Sitkowski, Matthew & Kossin, James & Rozoff, Christopher. (2011). Intensity and Structure Changes during Hurricane Eyewall Replacement Cycles. Monthly Weather Review. 139. 3829-3847. 10.1175/MWR-D-11-00034.1.

Willoughby, H. E., Clos, J. A., & Shoreibah, M. G. (1982). Concentric Eye Walls, Secondary Wind Maxima, and The Evolution of the Hurricane vortex, *Journal of Atmospheric Sciences*, *39*(2), 395-411. Retrieved Feb 2, 2022, from https://journals.ametsoc.org/view/journals/atsc/39/2/1520-0469_1982_039_0395_cewswm_2_0_co_2.xml

Wunsch, K. E. D., & Didlake, A. C., Jr. (2018). Analyzing Tropical Cyclone Structures during Secondary Eyewall Formation Using Aircraft in Situ Observations, *Monthly Weather Review*, 146(12), 3977-3993. Retrieved Dec 19, 2022, from https://journals.ametsoc.org/view/journals/mwre/146/12/mwr-d-18-0197.1.xml

Yang, Y.-T., Kuo, H.-C., Tsujino, S., Chen, B.-F., & Peng, M. S. (2021). Characteristics of the long-lived concentric eyewalls in tropical cyclones. *Journal of Geophysical Research: Atmospheres*, 126, e2020JD033703. https://doi.org/10.1029/2020JD033703

Zhou, Xiaqiong, & Wang, Bin. (2011). Mechanism of Concentric Eyewall Replacement Cycles and Associated Intensity Change*. *Journal of the Atmospheric Sciences*, vol. 68, no. 5, 2011, pp. 972–988., doi:10.1175/2011jas3575.1

ACADEMIC VITA
Martha Lisbeth Christino

Education

The Pennsylvania State University - May 2023

> Bachelor of Science in Meteorology and Bachelor of Science in Civil Engineering
>
> Schreyer Honors College
>
> Phi Beta Kappa

The University of Virginia – August 2018

> UVA Advance Summer Program
>
> Introduction to Oceanography
>
> Credit Received for Interdisciplinary Studies (Research in Mechanical Engineering)

Awards/Recognitions

> *University Awards*
>
> 2022 - The Pennsylvania State University Evan Pugh Scholar Award (Top 0.5% of the University)
>
> 2022 – Selected as the Department of Meteorology and Atmospheric Sciences Nominee to the National Center for Atmospheric Research Undergraduate Leadership Workshop
>
> 2021 – Elected to Phi Beta Kappa
>
> 2021 - The Pennsylvania State University President's Sparks Award
>
> 2020 - The Pennsylvania State University President's Freshman Award
>
> *Air Force ROTC Awards/Recognitions*
>
> 2022 – Selected as Air Force ROTC North-East Region Delegate to the National Character and Leadership Symposium
>
> 2019/2021 - Five-time recipient of the Air Force ROTC Meritorious Service Award (award given to the top 5% of the ROTC class)
>
> 2021 - Air Force ROTC Scottish Rite Southern Jurisdiction Award
>
> 2020 - Air Force ROTC American Legion Scholastic Excellence Award
>
> 2020 – Elected to the Tri-Service Honor Society (Scabbard and Blade)
>
> *Scholarships*
>
> 2022/23 Academic Year – College of Earth and Mineral Sciences Matthew J. Wilson Honors Scholarship
>
> 2022/23 and 2021/22 Academic Year - Department of Civil and Environmental Engineering Walter J. Kinsey Honors Scholarship
>
> 2022/23 and 2021/22 Academic Years - Robert Case Memorial Scholarship for Meteorology Students
>
> 2021/22 Academic Year - College of Earth and Mineral Sciences Marie Radomsky and Vernon W. Ellzey Honors Scholarship
>
> 2019 - Schreyer Honors College Academic Excellence Scholarship
>
> 2018 - Virginia Environmental Endowment France A. Lewis and Sydney Lewis Environmental Science Scholarship

Research Experience

Undergraduate Researcher, Penn State College of Earth and Mineral Sciences – June 2020/Present

Research for undergraduate honors thesis in predicting the Eyewall Replacement Cycle (ERC) of Hurricanes. Currently working on determining the environmental factors that influence the Eyewall Replacement Cycle of hurricanes through statistical analysis of change in predictor variables before ERC events. Selected variables will be used in a machine learning program to predict ERC development.

Solar Irradiance for Special Operations Power Generation Capstone Project, Penn State College of Earth and Mineral Science – January/May 2022

Deployed low-cost solar irradiance sensors along a valley and ridge to study the feasibility of using similar sensors to determine available solar power supply for special operations units in mountainous areas.

Metacognition in Tactical Level Leadership Undergraduate Honors Project, Penn State Schreyer Honors College- August/December 2020

Analysis of required skills for military tactical level leaders based on published works. Examined common theme of the need for metacognition in tactical level leaders and explored possible options for implementing metacognition training in officer accessions routes.

Trauma and Leadership Development Undergraduate Honors Project, Penn State Schreyer Honors College – January/May 2022

Examined modern literature on the impact of traumatic experience on a leader's ability to exemplify transformational leadership. Combined published works with interview of crew from Operation Allies Refuge to explore how effectively the United States Air Force prepares officers to lead during and after traumatic experiences.

Research Assistant, Flow Simulation Research Group, University of Virginia – July/August 2018

Created skeletal structures in Autodesk Maya and mesh overlays for computational fluid dynamics (CFD) and modeled CFD outputs for three-dimensional printing.

Work Experience

Intern, The Whiting-Turner Contracting Company – June/August 2021, May/July 2022

Led team in Leadership in Energy and Environmental Design (LEED) reporting, working in tandem with a third-party organization responsible for sustainable building at the University of Maryland. Responsible for the development of construction site work plans to mitigate the impact of development on local aquifers at Pennsylvania State University.

Skills: collaboration, communication, problem-solving, presenting

Intern, Penn State College of Engineering Bernard M. Gordon Learning Factory- June/August 2020

Managed team running web development Designed College of Engineering Learning Factory @Home. Created Diversity and Inclusion micro-credential course for College of Engineering by leading group of faculty and students.

Skills: leadership, web-design, public-speaking

Intern, MPR Engineering Associates – June 2019

Assisted with Piping and Instrumentation Diagram analysis for pipe schedule and stress calculations. Performed tornado missile calculations of nuclear power plant design to ensure safety during natural disasters.

Skills: understanding of design code, communication

United States Senate Page – June/August 2018

Nationally selected to be part of the United States Senate Page Program. Severed standard summer page term in June and was asked to return to cover a special session of congress in August. Selected as Page to carry presidential nominations prior to announcement.

Publications

"Analysis of Environmental Factors Contributing to the Eyewall Replacement Cycle of Hurricanes." Research presented at the *American Meteorological Society Annual Meeting*, Denver, CO. Jan 8, 2023.

"Analysis of Environmental Factors Contributing to the Eyewall Replacement Cycle of Hurricanes." Research presented at the *Great Lakes Atmospheric Science Symposium,* Oswego, NY. Nov 5, 2022.

Wang, Junshi, Tran, Huy, **Christino, Martha**, White, Carl, Zhu, Joseph, Lauder, George, Bart-Smith, Hilary, and Dong, Haibo. "Hydrodynamics and Flow Characterization of Tuna-Inspired Propulsion in Forward Swimming." *Proceedings of the ASME-JSME-KSME 2019 8th Joint Fluids Engineering Conference. Volume 1: Fluid Mechanics*. San Francisco, California, USA. July 28–August 1, 2019. V001T01A025. ASME.

"Diagnosing and Predicting the Eyewall Replacement Cycle: Learning from Hurricane Irma." Research presented at the *Symposium on Data Science and Statistics*, Reston, VA. May 17, 2018.

Air Force Reserve Officer Training Corps Experience

Operations Division Commander – May 2022/Present

Responsible for 16 cadet officers and 33 underclassman cadets, in charge of planning and execution for over 10,000 training hours across the Cadet Delta.

President, Aerospace Studies Student Organization – May 2020/May 2022

Managed over $20K for 15 events impacting three regional Air Force ROTC detachments, led six-member team. Created Detachment scholarship program, facilitated awarding $3500 to seven cadets.

Wagner Cup Officer – December 2021/May 2022

Coordinated joint service morale competition between Army, Navy, and Air Force ROTC at Penn State including seven events and over 500 cadets/midshipmen.

Professional Officer Course Leadership Laboratory Officer - May/December 2021

Designed training curriculum for cadets preparing to enter active duty, including working with ten Penn State University professors for 207 training hours centered around understanding global conflicts.